Near-Minimum-Time Control of Distributed Parameter Systems: Analytical and Experimental Results

J. L. Junkins,* Z. H. Rahman,† and H. Bang‡
Texas A&M University, College Station, Texas 77843

We present a method for generating globally stable feedback control laws for maneuvers of distributed parameter structural systems. The method can accommodate system nonlinearity, and our proof of Lyapunov stability does not rely upon spatially discretizing distributed parameter systems. The approach applies directly to controllable distributed parameter systems that are open-loop conservative or dissipative. The most fundamental version of the formulation leads to controls that drive the system to a fixed point in the state space, but more generally, we develop tracking-type control laws to null the departure of the system state from a smooth target trajectory. Both analytical developments and experimental results are presented. The analytical results provide a theoretical foundation for the approach, whereas the experimental results provide conclusive evidence that the approach can be efficiently realized in actual hardware.

Nomenclature

EI	=	assumed constant bending stiffness of beams
I_1,I_2,I_3	=	principal moments of inertia
l,l_o	=	distance from the hub center to the beam tip and hub radius
M_o,S_o	=	root bending moment and shear force, respectively, at the hub clamp
m	=	mass of the tip mass
q_1,q_2,q_3	=	Euler-Rodriguez parameters
T	=	kinetic energy of rotation
t_f	=	maneuver time
$u_{\max}$	=	saturation torque
u_1,u_2,u_3	=	principal axis components of the external control torque
Δt	=	rise time = αt_f
θ	=	hub inertial rotation
ρ	=	assumed constant mass/unit length of beams
$\omega_1,\omega_2,\omega_3$	=	principal axis components of angular velocity

Introduction: Motivation of the Approach Using Rigid Body Maneuvers

THE ideas are easily introduced by first considering general, three-dimensional, nonlinear maneuvers of a single rigid body. The equations of motion are[1]

$$I_1\dot{\omega}_1 = (I_2 - I_3)\omega_2\omega_3 + u_1$$

$$2\dot{q}_1 = \omega_1 - \omega_2 q_3 + \omega_3 q_2 + q_1(q_1\omega_1 + q_2\omega_2 + q_3\omega_3)$$

$$I_2\dot{\omega}_2 = (I_3 - I_1)\omega_3\omega_1 + u_2$$

$$2\dot{q}_2 = \omega_2 - \omega_3 q_1 + \omega_1 q_3 + q_2(q_1\omega_1 + q_2\omega_2 + q_3\omega_3)$$

$$I_3\dot{\omega}_3 = (I_1 - I_2)\omega_1\omega_2 + u_3$$

$$2\dot{q}_3 = \omega_3 - \omega_1 q_2 + \omega_2 q_1 + q_3(q_1\omega_1 + q_2\omega_2 + q_3\omega_3) \qquad (1)$$

For the case of zero control torque, it can be verified readily that total rotational kinetic energy is an exact integral of the motion, viz., $2T = (I_1\omega_1^2 + I_2\omega_2^2 + I_3\omega_3^2) = \text{const}$. Motivated by this total system energy integral, we investigate the trial Lyapunov function

$$U = \tfrac{1}{2}(I_1\omega_1^2 + I_2\omega_2^2 + I_3\omega_3^2) + A(q_1^2 + q_2^2 + q_3^2) \qquad (2)$$

It is apparent that the additive term $A(q_1^2 + q_2^2 + q_3^2)$ can be thought of as the potential energy stored in a nonlinear spring; therefore, we might anticipate that the system dynamics will remain conservative if the only external torque is a conservative torsional spring. (Note that A is an arbitrary positive constant.) Of course, we are not interested in preserving U as a constant, but rather we seek to drive it to zero, and so we anticipate determination of a judicious nonconservative control moment to guarantee that U is a decreasing function of time. It is obvious by inspection that U is positive definite except at the desired state $q_i = \omega_i = 0$. Differentiation of Eq. (2) and substitution of Eqs. (1) leads directly to the following expression for $\dot{U}$:

$$\dot{U} = \sum_{i=1}^{3} \omega_i[u_i + Aq_i(1 + q_1^2 + q_2^2 + q_3^2)] \qquad (3)$$

Of the infinity of possible control laws, we can see that any $u_i(q_1, q_2, q_3, \omega_1, \omega_2, \omega_3)$ that reduces the bracketed terms to a negative semidefinite function times ω_i will guarantee that $\dot{U}$ is negative semidefinite. The simplest choice is to select u_i so that the ith bracketed term becomes $-k_i\omega_i$. This gives the negative semidefinite dissipation rate of $\dot{U} = -(k_1\omega_1^2 + k_2\omega_2^2 + k_3\omega_3^2)$, with $k_i > 0$. Thus, we obtain an elegant, globally stabilizing nonlinear feedback control law for large angle attitude control:

$$u_i = -[k_i\omega_i + Aq_i(1 + q_1^2 + q_2^2 + q_3^2)], \quad i = 1,2,3 \qquad (4)$$

Since U is a positive-definite, nonincreasing function of time that vanishes at the origin, then the necessary and sufficient conditions are satisfied for global Lyapunov stability. (Note that this control law guarantees stability of the nonlinear closed-loop system, of course, under the assumption of zero model errors.) Since $\dot{U}$ is only negative semidefinite, additional insight is required to conclude that we do indeed have asymptotic stability. This insight can be gained by substituting the control law of Eq. (4) into Eqs. (1) and verifying that the only equilibrium point is the origin. Thus, angular velocity is generally nonzero for all $q_i(t)$ motions, and $\dot{U}$ is,

Received Oct. 2, 1989; revision received Feb. 1, 1990.

*George Eppright Professor, Department of Aerospace Engineering.
†Research Engineer, Department of Aerospace Engineering.
‡Graduate Research Assistant, Department of Aerospace Engineering.

therefore, negative almost everywhere (except at hub oscillation direction reversals and as it asymptotically approaches zero at the origin). We note that this discussion excludes the geometric singularity corresponding to a principal rotation angle of 180 deg. This law has been generalized, however, to permit feedback on the four Euler (quaternion) parameters as in Refs. 3 and 9, which results in globally nonsingular attitude control of a rigid body. The subsequent developments in this paper establish similar, globally stabilizing maneuver control laws for near-minimum-time, single-axis, flexible body maneuvers.

In practice, of course, guaranteed stability in the presence of zero model error is not a sufficient condition to guarantee stability of the actual plant with arbitrary model errors and disturbances. On the other hand, defining a region in gain space guaranteeing global stability for our best model of the nonlinear system is an important step; one can thereby restrict the optimization of gains to this stable family. The determination of the particular gain values can then be selected from the infinity of globally stabilizing gains based upon performance optimization criteria that take into account disturbance torque characterization, low sensitivity to model errors, desired system time constants, actuator saturation, and bandwith limitations. Note that any additional model approximations introduced in the gain design process cannot destabilize the nonlinear system (assuming, of course, that our nonlinear equations correctly model the system), so long as we restrict the feedback gains to lie in the stable region. In this case, we simply require $\{A, k_1, k_2, k_3\}$ to be positive. Of course, approximations used in the gain design process will usually degrade the performance of the actual nonlinear distributed parameter system vis-à-vis predictions based on the approximate models resulting from spatial discretizations and linearizations and, naturally, the painful truth that our best nonlinear model never prefectly captures the actual system's physics.

Notice that if a system has no inherent stiffness with respect to rigid body displacements, it is necessary to augment the energy integral by an artificial potential term such as $A(q_1^2 + q_2^2 + q_3^2)$ in the preceding example. Generally speaking, such terms should be introduced subject to the necessary condition that the target state is the global minimum of the modified energy function. Then, the controls are usually selected as simply as possible (from an implementation point of view) to force dissipation ($\dot{U} \leq 0$) of the modified energy (Lyapunov) function and thereby guarantee closed-loop stability. Control laws established by this approach are sometimes overly conservative, and so care must be taken that performance optimality is not sacrificed on the alter of global stability! We will see later that it is possible to relatively weight the subsets of the "error" energy associated with motion of structural subsystems, and, also, we will generalize the ideas to admit "error" energies measured from time varying target trajectories. The resulting flexibility of the approach provides freedom for choosing Lyapunov functions that are qualitatively comparable to the freedom of performance index selection for applying optimal control theory. Although generalizations of the distributed parameter systems might be approached in abstract terms, it is more illuminating to consider a specific distributed parameter system, as discussed in the following.

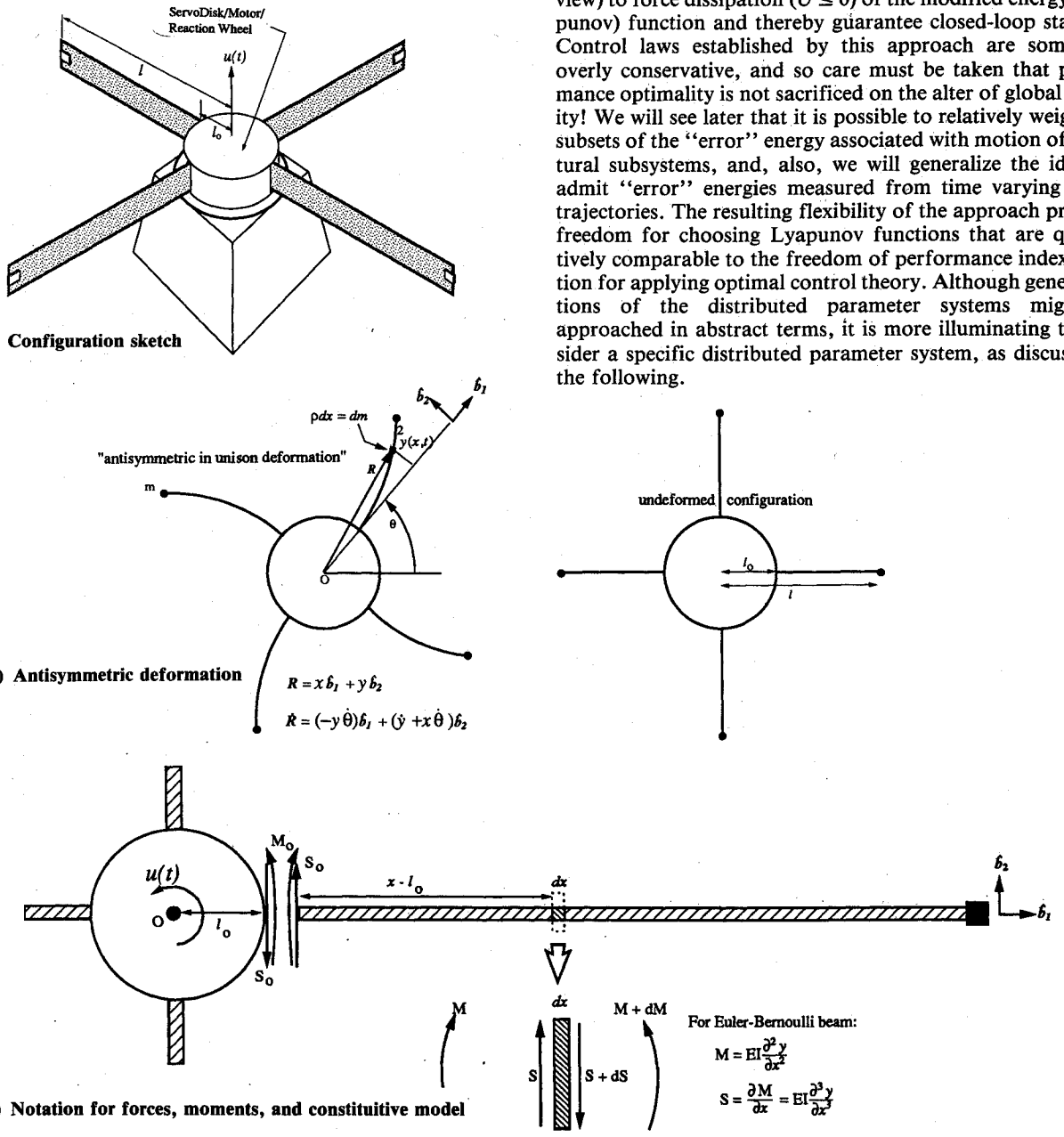

Fig. 1 Experimental configuration.

Vibration Suppression and Fine Pointing of a Distributed Parameter System

With reference to Figs. 1–3 and Table 1, we consider control of a rigid hub with four cantilevered flexible appendages. We consider the appendages to be identical uniform flexible beams and make the Euler-Bernoulli assumptions of negligible shear deformation and rotary inertia. Each beam is cantilevered rigidly to the hub and has a fine tip mass. Motion is restricted to the horizontal plane; a reaction wheel actuator generates control torque $u(t)$ that acts on the hub and is the only external effect considered. We are interested in a class of rest-to-rest maneuvers, and under the preceding assumptions, we can show that the beams will deform in the antisymmetric fashion (Fig. 1b) with the configuration's instantaneous mass center remaining at the hub's geometrical center. Also, due to the antisymmetric deformation of the beams, we need concern ourselves with the deformation $y(x,t)$ of a single beam. The hybrid system of ordinary and partial differential equations governing the dynamics of this system are

$$I_{\text{hub}}\frac{\mathrm{d}^2\theta}{\mathrm{d}t^2} = u + 4(M_o - S_o l_o) \tag{5a}$$

$$-(M_o - S_o l_o) = \int_{l_o}^{l} \rho x\left(\frac{\partial^2 y}{\partial t^2} + x\frac{\mathrm{d}^2\theta}{\mathrm{d}t^2}\right)\mathrm{d}x + ml\left(l\frac{\mathrm{d}^2\theta}{\mathrm{d}t^2} + \frac{\partial^2 y}{\partial t^2}\bigg|_l\right) + \text{HOT} \tag{5b}$$

$$\rho\left(\frac{\partial^2 y}{\partial t^2} + x\frac{\mathrm{d}^2\theta}{\mathrm{d}t^2}\right) + EI\frac{\partial^4 y}{\partial x^4} = 0 + \text{HOT} \tag{5c}$$

We denote higher-order terms by HOT to indicate other known linear and nonlinear effects (such as rotational stiffening, shear deformation, extensional deformation, etc.). Most of the developments herein do not consider these higher-order effects, however, we selectively discuss these generalizations as well. The boundary conditions on Eqs. (5) are

At $x = l_o$:

$$y(t,l_o) = \frac{\partial y}{\partial x}\bigg|_{l_o} = 0 \tag{6a}$$

At $x = l$:

$$\frac{\partial^2 y}{\partial x^2}\bigg|_l = 0 \text{ (zero moment)} \tag{6b}$$

$$\frac{\partial^3 y}{\partial x^3}\bigg|_l = \frac{m}{EI}\left(l\frac{\mathrm{d}^2\theta}{\mathrm{d}t^2} + \frac{\partial^2 y}{\partial t^2}\bigg|_l\right)\text{(shear force)} \tag{6c}$$

The total energy of the system (which is constant in the absence of control or disturbances)

$$2E = I_{\text{hub}}\left(\frac{\mathrm{d}\theta}{\mathrm{d}t}\right)^2 + 4\left[\int_{l_o}^{l}\rho\left(\frac{\partial y}{\partial t} + x\frac{\mathrm{d}\theta}{\mathrm{d}t}\right)^2\mathrm{d}x + \int_{l_o}^{l} EI\left(\frac{\partial^2 y}{\partial x^2}\right)^2\mathrm{d}x + m\left(l\frac{\mathrm{d}\theta}{\mathrm{d}t} + \frac{\partial y}{\partial t}\bigg|_l\right)^2\right] \tag{7}$$

Motivated by the recent work of Fujii et al.[5] and Vadali,[9] we investigate the Lyapunov function

$$2U = a_l I_{\text{hub}}\dot{\theta}^2 + a_2(\theta - \theta_f)^2 + 4a_3\left[\int_{l_o}^{l}\rho\left(\frac{\partial y}{\partial t} + x\dot{\theta}\right)^2\mathrm{d}x + \int_{l_o}^{l} EI\left(\frac{\partial^2 y}{\partial x^2}\right)^2\mathrm{d}x + m\left(l\dot{\theta} + \frac{\partial y}{\partial t}\bigg|_l\right)^2\right] \tag{8}$$

where the coefficients a_i are included to allow relative emphasis on the three contributors to the error energy of the system, and $(\dot{}) \equiv (\mathrm{d}/\mathrm{d}t)$. We have added the rigid body spring energy term $a_2(\theta - \theta_f)^2$ to make the desired final state

$$\left[\theta, \dot{\theta}, y(x,t), \frac{\partial y(x,t)}{\partial t}\right]_{\text{desired}} = (\theta_f, 0, 0, 0)$$

be the global minimum of U. It is obvious by inspection that choosing $a_i > 0$ guarantees that $U \geq 0$, and that, indeed, the global minimum of $U = 0$ occurs only at the desired state.

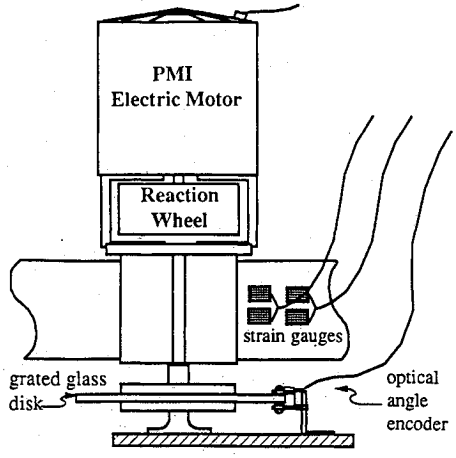

Fig. 2 Hub assembly.

Table 1 Air Force Office of Scientific Research/ Texas A&M University configuration parameters

Total undeformed system inertia, I	2128, oz-s^2-in.
Hub center to gauge center, l_o	5.5470, in.
Hub center to tip mass, l	51.07, in.
Tip mass, m	0.15627, oz-s^2/in.
Appendage modules of elasticity, E	161.6×10^6, oz/in.^{2}
Inertia of bending section, I	0.000813, in.^{4}
Mass density of appendage/length, ρ	0.003007, oz-s^2/in.^{2}
Distance between two strain gauge set	1.365, in.

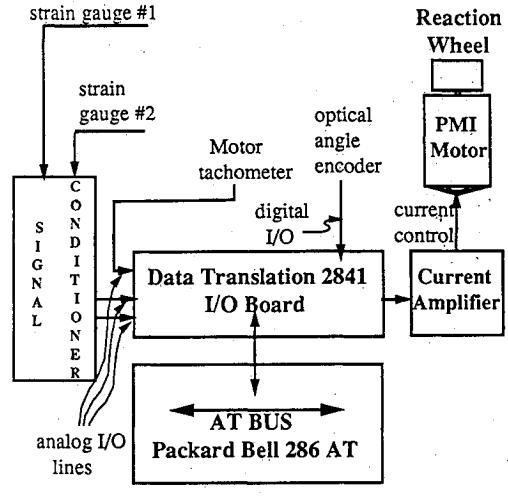

Fig. 3 System functional block diagram.

Differentiation, substitution of the equations of motion [Eqs. (5) and (6)], and some calculus lead to

$$\dot{U} = \frac{dU}{dt} = \dot{\theta}[a_1 u + a_2(\theta - \theta_f) + 4(a_3 - a_1)(l_o S_o - M_o)] \quad (9)$$

Since we require that $\dot{U} \leq 0$ to guarantee stability, we choose the control torque u as

$$u = -(1/a_1)[a_2(\theta - \theta_f) + a_4\dot{\theta} + 4(a_3 - a_1)(l_o S_o - M_o)] \quad (10)$$

so that $\dot{U} = -a_4\dot{\theta}^2$, and we obtain the following globally stabilizing output feedback law

$$u = -\left[g_1(\theta - \theta_f) + g_2\dot{\theta} + g_3(l_o S_o - M_o)\right]$$
$$g_1 \geq 0, \quad g_2 \geq 0, \quad g_3 > -4, \quad \text{for stability} \quad (11)$$

This control law is elegant. Notice that global stability of the distributed parameter system is guaranteed, and since this is an output feedback law, no state estimation is required. The root shear and bending moment can be measured by (albeit somewhat noisy) conventional strain gauges. The sign of $g_3 = 4(a_3 - a_1)/a_1$ depends whether we wish to emphasize dissipation of the beam energy $a_3 > a_1$ or suppress the motion of the hub $a_3 < a_1$, as is evident from Eq. (8). The limit of $g_3 \Rightarrow -4$ is approached as $a_3 \Rightarrow 0$, in which case the strongest emphasis is placed on arresting the hub vibration. Since $\dot{U} = -a_4\dot{\theta}^2$ is only negative semidefinite, proof of asymptotic stability rests on the truth that all infinity of modes of this system, under the implicit constraint of antisymmetric deformation, can be shown to have nonzero hub rotation. The eigenfunctions are established in Ref. 15. Therefore, $\dot{\theta}(t)$ cannot vanish identically unless $y(x,t)$ and $[\theta(t) - \theta_f]$ are identically zero, and as a consequence, $\dot{U} = -a_4\dot{\theta}^2 \leq 0$ and cannot vanish identically until the desired state has been achieved. We therefore have global asymptotic stability.

It is of significance that this same linear feedback law, Eq. (11), maintains its globally stabilizing character even when the Euler-Bernoulli assumptions are generalized to include the additional linear and nonlinear terms associated with the following effects: rotational stiffening, coriolis kinematic coupling terms, aerodynamic drag, shear deformation, rotary inertia of the beam, and the finite inertia of the tip mass. The proof of these truths requires that the kinetic and potential energy terms be modified to include these effects and that the differential equations of motion be generalized consistently. In short, global stability of the system using the control law of Eq. (11) is very forgiving of modeling assumptions and, therefore, modeling errors.

A key necessary condition, which underlies the existence of globally stabilizing control for the present application, and envisioned extensions to more general distributed parameter systems, is that the system must be controllable. Thus, the fact that all infinity of the modes of Eqs. (5) are controllable by the single input $u(t)$ is a key necessary condition underlying the existence of the globally stabilizing control law of Eq. (11) and the extensions to the stable tracking laws of Eqs. (17) and (20) developed in the following section. For a flexible body system to be controllable, it is necessary that the number of actuators be at least equal to the number of rigid body freedoms of the system. Thus truth can be inferred by the near-trivial observation that the flexible body model always includes a rigid body as a limiting special case.

Although the constant gain linear feedback of Eq. (11) can be tuned to work well for terminal pointing and vibration suppression, it is a poor law for carrying out both a large angle maneuver and terminal pointing/vibration suppression. In fact, it quickly becomes evident from either analytical/numerical or experimental studies that sophisticated gain schedule is required if we use the linear feedback law of Eq. (11) to efficiently control both the large maneuvering motions and the small terminal motions. This is because the large gains required for effective vibration suppression near the target state are typically several orders of magnitude too large for near-minimum-time large angle maneuvers (i.e., the large gains appropriate for vibration suppression, when used during a large angle maneuver, typically results in significant θ overshoots and, often, actuator saturation). Also, the large initial torque typically introduces a large transient into the structure. To obtain a control law appropriate for near-minimum-time large angle maneuvers with vibration suppression, we modified the preceding developments to obtain stable tracking-type feedback control laws. These results, including discussion of global stability, are presented in the following section.

Near-Minimum-Time Large Angle Maneuvers of a Distributed Parameter System

Consider briefly the near-minimum-time maneuver of a rigid body. We know that the strict minimum-time control is a bang-bang law, which for the rest-to-rest maneuver-to-the-origin case, saturates negatively during the first half of the maneuver and positively during the last half of the maneuver.[1,11-14] From an implementation point of view, the instantaneous switches of the bang-bang law are troublesome because 1) no torque-generating device exists that can switch instantaneously; 2) when generalized and applied to a flexible structure, the bang-bang class of controls excite poorly modeled higher modes; and 3) the switch times (and, therefore, the response of actual system) are usually very sensitive to modeling errors. Recently, an attractive family of controllably smooth approximations of the sign function has been introduced to modify the admissible controls in minimum-time control formulations. The approximation we presented in Refs. 8 and 10 involves products of transcendental functions, but our recent experimental work[2,7] indicates that a much simpler piecewise continuous spline approximation of the sign function is more attractive from an implementation point of view. Using this approach, a typical near-minimum-time control law (for single axis, rest-to-rest maneuver of a rigid body) has the form

$$I\ddot{\theta} = u = \pm u_{\max} f(\Delta t, t_f, t) \quad (12)$$

where t_f is the maneuver time, we choose the + sign if $\theta_f > \theta_o$, $\alpha = \Delta t/t_f$, and the smooth sign function approximation adopted is

$$f(\Delta t, t_f, t) \begin{cases} = \left(\frac{t}{\Delta t}\right)^2\left[3 - 2\left(\frac{t}{\Delta t}\right)\right], & \text{for } 0 \leq t \leq \Delta t \\ = 1 & \text{for } \Delta t \leq t \leq \frac{t_f}{2} - \Delta t \equiv t_1 \\ = 1 - 2\left\{\left(\frac{t - t_l}{2\Delta t}\right)^2\left[3 - 2\left(\frac{t - t_l}{2\Delta t}\right)\right]\right\}, & \text{for } t_1 \leq t \leq \frac{t_f}{2} + \Delta t \equiv t_2 \\ = -1 & \text{for } t_2 \leq t \leq t_f - \Delta t \equiv t_3 \\ = -1 + \left(\frac{t - t_3}{\Delta t}\right)^2\left[3 - 2\left(\frac{t - t_3}{\Delta t}\right)\right], & \text{for } t_3 \leq t \leq t_f \end{cases}$$

Adopting the positive sign, Eq. (12) integrates to yield

$$\dot{\theta}(t) = \dot{\theta}_o + \frac{u_{\max}}{I}\int_{t_o}^{t} f(\Delta t,\ t_f, \tau)\mathrm{d}\tau \tag{13a}$$

$$\theta(t) = \theta_o + (t - t_o)\dot{\theta}_o + \frac{u_{\max}}{I}\int_{t_o}^{t}\int_{t_o}^{\tau 1} f(\Delta t, t_f, \tau_2)\mathrm{d}\tau_2\mathrm{d}\tau_1 \tag{13b}$$

The integrations in Eqs. (13) can be carried out in terms of elementary functions, which are not presented here for the sake of brevity. Figure 4 shows a maneuver resulting from these integrations for a typical selection of parameters ($\alpha = 0.25$, $u_{\max} = 400$ oz-in., and a 40 deg rest-to-rest maneuver of a rigid approximation of the structure in Fig. 1 and Table 1). For rest-to-rest maneuvers, we impose the boundary conditions.

At $t_o = 0$:

$$\theta(0) = \theta_o, \qquad \dot{\theta}(0) = 0 \tag{14a}$$

At time t_f:

$$\theta(t_f) = \theta_f, \qquad \dot{\theta}(t_f) = 0 \tag{14b}$$

and upon carrying out the integrations implied in Eqs. (13), we obtain the useful relationship

$$\theta_f - \theta_o = \left(\frac{u_{\max}}{I}\right)\left[\frac{1}{4} - \frac{1}{2}\alpha + \frac{1}{10}\alpha^2\right]t_f^2$$

$$\Delta t = \alpha t_f, \qquad 0 < \alpha < (1/4) \tag{15}$$

or

$$t_f = \left\{\frac{I(\theta_f - \theta_o)}{u_{\max}[(1/4) - (1/2)\alpha + (1/10)\alpha^2]}\right\}^{1/2} \tag{16}$$

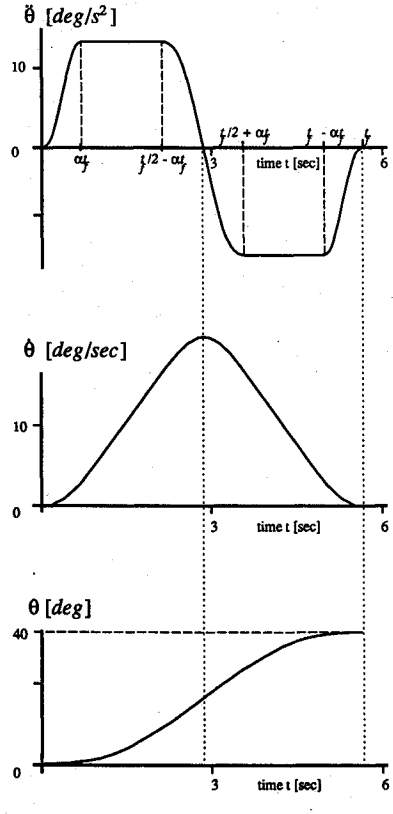

Fig. 4 Torque-shaped rigid body maneuver.

In Eq. (16), we have the explicit tradeoff between torque shaping α, target maneuver time t_f, maneuver angle $\theta_f - \theta_o$, and maximum angular acceleration $u_{\max}/I$. Obviously, Eqs. (15) can be inverted for any of these as a function of the remaining parameters. If we set $\alpha = \Delta t/t_f = 0$, of course, we obtain the well-known special case result expressing the relationship between the minimum time, maneuver angle, inertia, and saturation torque for bang-bang control. It is obvious that setting α controls the sharpness of the switches, with $\alpha = 0$ corresponding to bang-bang control (instantaneous switches). Figure 5 shows the maneuver time t_f vs α, from Eq. (16), whereas Fig. 6 shows the residual total energy (at time t_f) when the torque command $u_{\mathrm{ref}}(t) = u_{\max} f(\alpha t_f,\ t_f,\ t)$ is applied to simulate the flexible body response (first six modes from a discrete Ritz model[2] of order 20). Notice (Fig. 6) that open-loop torque shaping reduces residual vibration at time t_f by 3 orders of magnitude ($\alpha = 0.1$) with only about a modest increase over the minimum time rigid body maneuver ($\alpha = 0$).

The preceding results and Refs. 6–10 support the intuitively obvious truth that applying judiciously smoothed bang-bang controls such as Eq. (12) to generate an open-loop maneuver

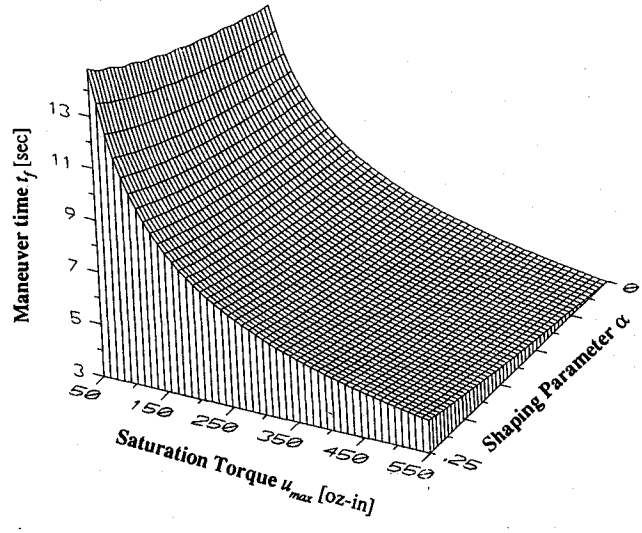

Fig. 5 Rigid body maneuver time vs saturation torque and torque-shaped parameter.

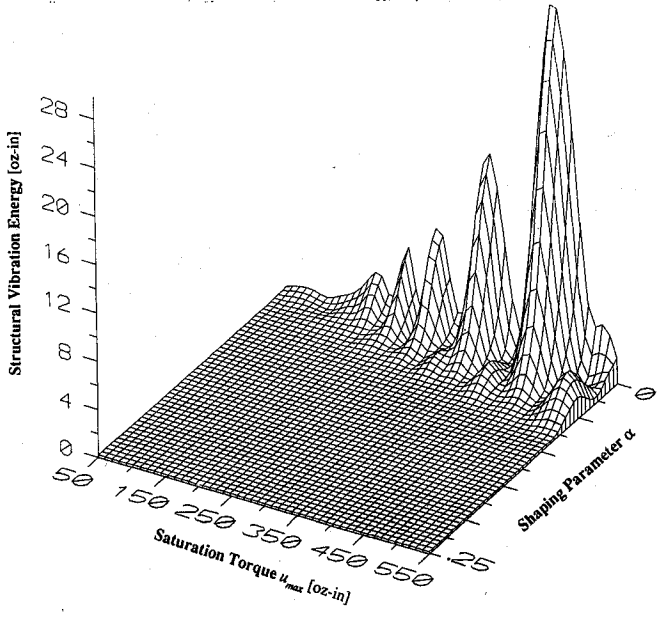

Fig. 6 Flexible body open-loop residual vibration energy vs saturation torque and torque-shaped parameter.

of a flexible body can result in near negligible structural vibration, for sufficiently slow maneuvers (small u_{max} and large α) and neglecting disturbance torques. Of course unmodeled disturbances, control implementation errors, and model errors will almost always negate some of these apparent gains. However, sharper control switches obviously increase the probability that higher frequency, less well-modeled models will be excited, and, therefore, robustness is generally even more of an issue for bang-bang controls. Even for relatively small departures from bang-bang control, actual torque-shaped maneuvers of highly flexible structures typically enjoy several orders of magnitude reduction in residual vibration, thus, overall maneuver time can be reduced significantly by torque shaping. This suggests the strategy of using a shaped torque profile to define an a priori reference rigid or flexible body maneuver, then based upon measurements of the actual flexible body's departure from this reference motion, superimpose a feedback control on the reference shaped torque history. Also of significance, it is usually desirable to select the reference torque profile (e.g., u_{max}, α, etc.) to consider the available sensor and actuator dynamics and thereby make the commanded torque history more nearly physically achievable.

Pursuing this logic judiciously, a family of tracking feedback control laws can be established for near-minimum-time, large angle maneuvers; these laws have a similar structure to the stable output feedback control of Eq. (11) and, in fact, approach it continuously as the maneuver is completed. Our approach is motivated by our analytical, numerical, and experimental results,[2,4,6-10] which indicate that bang-bang flexible body controllers are sensitive to modeling and control implementation errors. Thus, we seek control laws that are a smooth torque-shaped compromise between the competing objectives of 1) minimizing maneuver time, 2) minimizing residual vibration, and 3) minimizing sensitivity to model and control implementation errors.

Suppose we adopt a reference rigid body maneuver $\{\theta_{ref}(t), \dot{\theta}_{ref}(t), \ddot{\theta}_{ref}(t) = u_{ref}/I\}$ satisfying Eqs. (12-16), where I is the undeformed moment of inertia, and we have implicitly selected α, u_{max}, and computed t_f from Eq. (16) for specified initial and final angle. Motivated by the issues discussed earlier and the quadratic regulator perturbation feedback controllers discussed in Refs. 1 and 8, we hypothesize the following structure for the control law.

$$u = u_{ref}(t) - \{g_1(\theta - \theta_{ref}) + g_2(\dot{\theta} - \dot{\theta}_{ref}) + g_3[(l_oS_o - M_o) - (l_oS_o - M_o)_{ref}]\} \tag{17}$$

where it is easy to show that the root moment for the reference (rigid body) motion is proportional to the angular acceleration:

$$(l_oS_o - M_o)_{ref} = [\rho(l^3 - l_o^3) + ml^2]\ddot{\theta}_{ref}(t)$$

We consider the candidate error energy Lyapunov function

$$2U = a_1 I_{hub}\delta\dot{\theta}^2 + a_2\delta\theta^2 + 4a_3\left\{\int_{l_o}^{l}\rho\left[\delta\frac{\partial y}{\partial t} + x\delta\dot{\theta}\right]^2 dx + \int_{l_o}^{l} EI\left(\delta\frac{\partial^2 y}{\partial x^2}\right)^2 dx + m\left[l\delta\dot{\theta} + \delta\frac{\partial y}{\partial t}\bigg|_l\right]^2\right\} \tag{18}$$

Where $\delta(\,) \equiv (\,) - (\,)_r$ and the $(\,)_r$ quantities are evaluated along the open-loop flexible body solution of Eqs. (5) with $u(t) = u_{ref}(t)$. We have investigated the time derivative of U and found that it is given exactly by

$$\dot{U} = (\dot{\theta} - \dot{\theta}_r)\{a_1u - a_1u_{ref} + a_2(\theta - \theta_r) + 4(a_3 - a_1)[(l_oS_o - M_o) - (l_oS_o - M_o)_r]\} \tag{19}$$

Pursuing the objective of globally stable control, it is clear that setting the $\{\}$ term equal to $-a_4(\dot{\theta} - \dot{\theta}_r)$ leads to the following globally stabilizing [with $\dot{U} = -a_4(\dot{\theta} - \dot{\theta}_r)^2$] control law

$$u = u_{ref}(t) - \{g_1(\theta - \theta_r) + g_2(\dot{\theta} - \dot{\theta}_r) + g_3[(l_oS_o - M_o) - (l_oS_o - M_o)_r]\} \tag{20}$$

Obviously, the globally stabilizing control law of Eq. (20) is similar to the conjectured law of Eq. (17); the difference being that Eq. (17) requires presolution for the open-loop rigid body $(\,)_{ref}$ quantities, whereas the globally stabilizing control law of Eq. (20) requires solution for the open-loop flexible body $(\,)_r$ quantities from the partial differential equations. Since near-minimum-time control implies a certain urgency, it is obvious that the negligible computational overhead of Eq. (17) makes it more attractive than Eq, (20), from the point of view of real-time implementations. Therefore, the following question naturally arises: what are the global stability characteristics of the system using the simpler law of Eq. (17), as a function of the gains (g_1, g_2, g_3) and the torque shape parameters (α, u_{max}) implicit in $u_{ref}(t)$? Rather than using Eq. (19) to determine $u(t)$ of Eq. (20), we can instead use Eq. (19) to evaluate the stability of motion resulting from using the feedback control $u(t)$ of Eq. (17). The region possessing Lyapunov stability can be found directly by substituting Eq. (17) into Eq. (19) and finding the region for which $\dot{U}$ is guaranteed to be negative. Substitution of Eq. (17) into Eq. (19), upon introducing notation $\Delta(\,) = (\,)_r - (\,)_{ref}$, leads to

$$\dot{U} = -a_1(\dot{\theta} - \dot{\theta}_r)\{g_2(\dot{\theta} - \dot{\theta}_r) + [g_1\Delta\theta + g_2\Delta\dot{\theta} + g_3\Delta(l_oS_o - M_o)]\} \tag{21}$$

Notice that a sufficient condition characterizing the region where $\dot{U} \le 0$ is the dominance of the first term in the braces of Eq. (21), this gives the Lyapunov stability condition

$$|\dot{\theta} - \dot{\theta}_r| > \mu \equiv (1/g_2)|g_1\Delta\theta + g_2\Delta\dot{\theta} + g_3\Delta(l_oS_o - M_o)| \tag{22}$$

If the angular velocity tracking error $|\dot{\theta} - \dot{\theta}_r|$ exceeds μ, then $\dot{U}$ is negative and apparently U decreases until the region bounded by Eq. (22) is approached. It is further apparent that the Δ quantities on the right side of Eq. (22) are finite and (pre-) computable differenced between the open loop flexible $(\,)_r$ and rigid body $(\,)_{ref}$ motions; thus, an upper bound can be established directly by precomputation of a family of two open-loop motions and the use of a particular set of feedback gains. Equation (22) thus determines an angular velocity boundary defining a region Γ near the $(\,)_{ref}$ motion. Note that large motions are globally attracted to Γ because $\dot{U} \le 0$ everywhere outside of this region. Thus, the control law of Eq. (17) is almost globally stabilizing, and the only region where asymptotic stability cannot be guaranteed is in Γ near the target trajectory. Furthermore, the right side of Eq. (22) is essentially a measure of how nearly the target trajectory satisfies the flexible body equations of motion; a judicious choice of the torque shaping parameters defining the target trajectory can usually be made to result in μ being sufficiently small.

A bounded-input/bounded-output (BIBO) viewpoint of stability can be used to establish some insight into the motion in the Γ region. Departure motion differential equations for $\delta(\,) = (\,) - (\,)_r$ quantities can be obtained by differencing Eqs. (5), driven by the control law of Eq. (17), from the rigid body equations of motion, driven by $u_{ref}(t)$. Upon formulating these equations, we find departure motion is governed by a linear, otherwise asymptotically stable system of differential equation, forced by the known Δ terms that appear in Eq. (22). The $\delta(\,)$ motion in the Γ region is thus bounded because the Δ forcing terms are bounded; the finite maxima of these terms can be found by direct calculation. The resulting

departure motion is therefore bounded everywhere in the Γ region, which was already known to have a finite dimension μ. Since the actual numerical bounds on the Δ and μ quantities can be made arbitrarily small (depending on how nearly the user-defined reference trajectory is made to satisfy the open-loop equations of motion), we have a very attractive theoretical and practical situation vis-á-vis stability of the closed-loop tracking motion. We see that the closed-loop motion is globally attracted to the controllable small Γ region near the target trajectory, and considering the motions within Γ, we have BIBO stability.

The preceding discussion probably can be generalized for any smooth target trajectory, but we find that it is especially attractive to use a torque-shaped rigid body reference trajectory because the reference maneuver can be calculated in closed form [such as the family of Eqs. (12–16)]. Note that Eqs. (12–16) have a C^1 continuous transition to the final fixed state:

$$\left\{u_{\text{ref}}(t),\theta_{\text{ref}}(t),\dot{\theta}_{\text{ref}}(t),M_{o_{\text{ref}}}(t),S_{o_{\text{ref}}}(t)\right\} \Rightarrow \left\{0,\theta_f,0,0,0\right\} \quad as\ t \Rightarrow t_f$$

so that for $t > t_f$, only the three feedback terms of Eqs. (17) are contributing to the terminal fine-pointing/vibration arrest control. Thus, the controls blend continuously from the large angle tracking law of Eq. (17) into a constant gain controller (for $t > t_f$) identical to the globally stable fixed point output feedback case of Eq. (10).

Simulated Results for the Large Angle Maneuvers Experiment

Returning to the family of 40 deg open-loop maneuvers used to generate the energy surface of Fig. 6, we computed the velocity tracking bound μ for Lyapunov stability [as given by Eq. (22)] and found the maximum value ($\mu_{\max}$) of $\mu(t)$ along each trajectory. Figure 7 displays this worst case tracking bound (maximum value of μ) surface $\mu_{\max}$ (α, $u_{\max}$) region used to generate Fig. 5 and 6. The closed-loop tracking error bound has a roughly analogous behavior to the open-loop residual vibration energy surface of Fig 6. Recall that outside the region bounded by the inequality of Eq. (22) we have guaranteed Lyapunov stability, using the control law of Eq. (17) and the reference rigid body torque given by Eqs. (12–16). From Fig. 6, it is clear that sufficiently small $\mu_{\max}$ and large α result in arbitrarily small tracking errors, but the (small α, large $u_{\max}$) near-bang reference maneuvers cannot be tracked as precisely. It is easy to see how a family of candidate (α, $u_{\max}$) designs can be found that satisfy specified inequalities on maneuver times, tracking errors, and residual vibration energy by direct examination of the surfaces of Fig. 5–7.

Our experience with simulations (and in the actual hardware implementations presented later and in Refs. 2, 6, and 7) support the conclusion that we can use these surfaces to establish a large region of feasible designs in the space of torque-shaped parameters and control gains. Optimization over the set of feasible designs should include consideration of the nature of disturbances to be rejected. Prior to discussing our experimental results, we present some further simulations to show state and control variables histories along typical trajectories of underlying the above surfaces. We include in these simulations the effects of disturbance torques in order to illustrate the effectiveness of controls in the presence of unmodeled effects. For simplicity, we consider here only the case of a 40 deg rest-to-rest maneuver, and set $u_{\max} = 400$ oz-in. for all cases.

For our computational and experimental studies, we consider two control laws: namely, the output feedback law (control law I) of Eq. (10), and the tracking-type feedback control law (control law II) of Eq. (17). Although control law II could be used with an arbitrary reference trajectory, we elect to specifically investigate the torque-shaped rigid body trajectories of Eqs. (12–16). The torque-shaped open-loop control

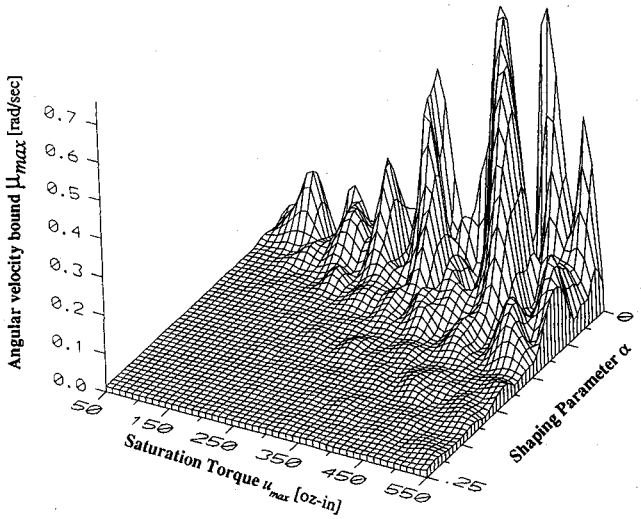

Fig. 7 Boundary of the Lyapunov-stable tracking region vs saturation torque and torque-shaped parameter.

history $u_{\text{ref}}(t)$ can be precomputed (in a fraction of a second!) from Eqs. (12–16) and stored, whereas the instantaneous trajectory variables $\{\theta_{\text{ref}}(t),\ \dot{\theta}_{\text{ref}}(t),\ [l_o S_o(t) - M_o(t)]_{\text{ref}}\}$ are integrated easily in real time. Note that the boundary conditions of Eqs. (14) are enforced by using Eq. (16) to compute the trajectory maneuver time as a function of the maneuver angle, saturation torque, and torque-shaped parameter.

We now discuss the simulation results using control law II, which obviously blends into control law I in the end game (for $t \geq t_f$). In the experimental results, we report maneuvers carried out by both control laws and we confine the simulation results to control law II. Both open-loop (all $g_i \equiv 0$) and closed-loop time histories of selected variables are shown in Figs. 8a–8d for a typical maneuver. Figures 8a and 8b show the hub angle and angular velocity for the case of an open-loop control and in the presence of substantial impulsive and quasirandom (5 oz-in., 1 σ) disturbance torques. It is evident that the disturbance torque history is very significant vis-à-vis our experimental hardware; however, certain nonrandom, nonlinear effects associated with the bearing friction cause disturbances that are correlated in time and are not well represented by the present white noise model of the disturbance torques. In spite of the substantial disturbance torques (Figs. 8a ad 8b), however, it is evident that our simulations indicate that the closed-loop flexible body dynamics in fact follows the near-minimum-time rigid body motion closely while effectively suppressing vibration (Figs. 8c and 8d). In addition to the variables graphed in Figs. 8, we confirmed that the energy of the first 10 modes was effectively suppressed. These simulated results are very consistent with the experimental results below and those presented in Ref. 2.

Experimental Results

In all of the experiments discussed in the following, we set the target final angle to 40 deg and $u_{\max} = 400$ oz-in. A detailed description of the hardware is given in Ref. 2. We overview the system as follows. The configuration (Fig. 13, Table 1) has a span of approximately 9 ft and has six natural frequencies below 20 Hz. The system is accurately balanced, and the four aluminum appendages' geometric, mass, and stiffness parameters are matched to high precision; the first three measured cantilevered natural frequencies of the four individual beams were found to be identical[16] to within 0.05 Hz.

With this design, the appendages vibrate almost exclusively in the horizontal plane; the hub is balanced on a custom-designed needle-jewel bearing that constrains the hub to rotate about the vertical axis. Our measurements confirmed that negligible out-of-plane motion occurred in our experiments,

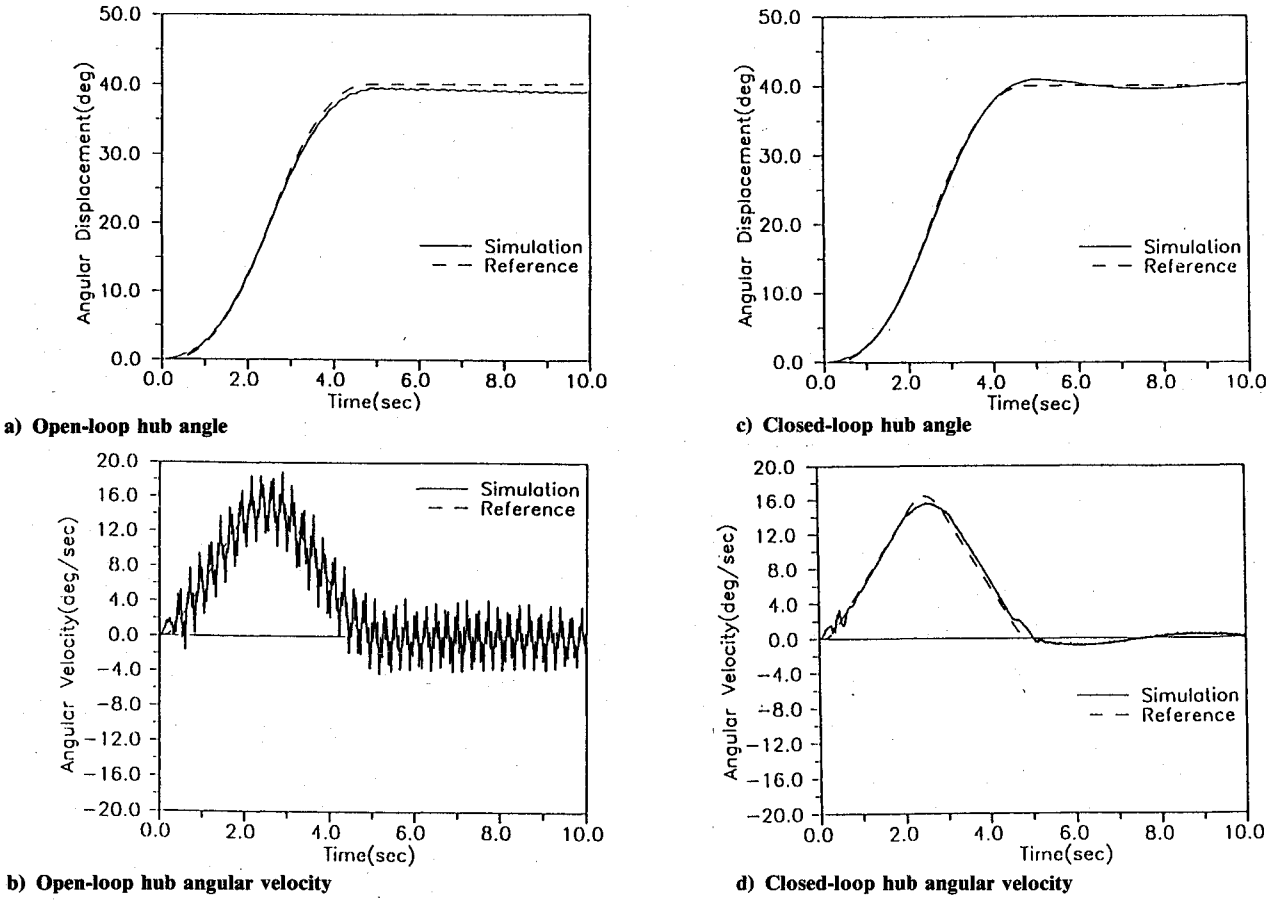

Fig. 8 Simulated open- and closed-loop 40-deg maneuver with random disturbance torques.

although there is occasional evidence of small beam torsional vibrations. The bearing stiction/friction torque is significant (~ 20 oz-in.), but is sufficiently small and predictable to permit meaningful experiments. Aerodynamic damping is important only during the most rapid slew maneuvers; it usually represents a small perturbation vis-à-vis the large active vibration damping introduced by the feedback controller. The control torque is achieved by means of a reaction wheel mounted to the shaft of a dc motor (Fig. 1c), which is, in turn, mounted to the hub. The commanded motor torque is achieved by precision current control using power amplifiers, as described in Ref. 2. The angular rotation of the hub is measured using a Teledyne-Gurley angle encoder accurate to about 0.01 deg, whereas the root bending moment and shear force estimates are derived from conventional full bridge strain angle measurements. The derived estimates of the angular velocity history has a variance of approximately 1 deg and a time lag of 0.01 sec. The noise and phase lags in the angular velocity estimates and the strain-gauge-derived root shear force and bending moment estimates limit the bandwidth of the closed-loop system to approximately 10 Hz. The errors in the noisy shear force and angular velocity estimates represent the main source of the precision and bandwith constraints of the experimental implementations. The control loops were closed, for all experiments discussed later, at 75 Hz; the angle encoder was also sampled at 75 Hz, whereas the strain gauges were sampled an order of magnitude faster and filtered to reduce the effects of sensor noise and higher frequency modes outside the bandwidth of our controller.[2]

Figure 9 shows the experimental system response for a maneuver using control law I [the constant gain control law of Eq. (11)] with $g_1 = 600$ oz-in./rad, $g_2 = 800$ oz-in./rad/s, and $g_3 = 0$. Even though control law I [Eq. (11)] is anticipated to be poorly designed for large angle maneuvers, we, nonetheless, apply this law to carry out 40 deg maneuvers to provide a reference for the subsequent discussion. Since the initial position error is large, the maneuver starts from zero with an initial discontinuity to a large torque. For this gain selection, we see a large overshoot (~ 10 deg) and significant structural vibration that settled around 12 s; the control was terminated at 16 s. These results were repeatable; however, the residual angle was typically ~ 0.25 deg because the gain g_1 could not be set sufficiently large to overcome terminal bearing stiction without causing initial actuator saturation and large overshoots. As is demonstrated in Ref. 2, the overall maneuver shape and settling time is sensitive to the gains selected; however, less than 10% reductions in the 12 s settling time can be achieved without initially saturating the actuator.

Control law II, on the other hand, leads to attractive near-minimum-time maneuvers. One feasible set of gain settings and torque shaped parameters leads to the experimental results shown in Fig. 10. The effect of using a smooth, judiciously shaped reference torque history is evident if one compares the output and control variable histories in Fig. 10 with those of Fig. 9. This implementation of control law II produced much smaller overshoot (≈ 1.5 deg vs ~ 10 deg), shorter maneuver time (6 s vs 12 s), and greatly reduced the severity of peak vibration, compared to control law I. These results, especially when considered in conjunction with numerous other cases, are reported in Refs. 2, 7, and 8 and provide convincing evidence that control law II is a versatile and highly effective way to incorporate open-loop torque shaped optimization with enroute and terminal vibration suppression. The fact that a globally continuous control structure is implicit in this approach leads to minimal difficulties in realizing robust control laws. We encountered several practical difficulties in our experimental work, but these difficulties are not central to our control law design approach. First, the shear force and bending moment measurements via strain gauges resulted in sufficiently noisy measurements that, using this feedback ($g_3 \neq 0$), only marginally improved the controlled response over, for example, the results in Fig. 10. Also, deriv-

ing the angular velocity estimate from the noisy angle encoder readout was difficult to accomplish with high precision, and as a consequence, we constructed a digital filter to process out angle encoder data and roll off the frequency content in the rate estimates above 10 Hz. We found this was useful to avoid erroneous, phase lagged high frequency components of the feedback that disturbed the higher frequency modes. This problem can be eliminated by investing in a more precise sensor to measure angular displacement and/or angular velocity. Finally, our bearing presented us with some mechanical difficulties. Based upon analysis of our bearing hardware, it became evident that interaction of the structure with the bearing accounts for the overwhelming source of disturbance torques. The bearing friction/stiction model developed from our analysis[2] has the form

$$\tau_{\text{bearing}} = -c_1 \text{ sign } (\dot{\theta}) - c_2\dot{\theta} + \text{HOT} \tag{23}$$

where we find $c_1 \sim 20$ oz-in. and $c_2 \sim 0.001$ oz-in./rad/s. Thus, the first (stiction) term of Eq. (23) dominates the bear-

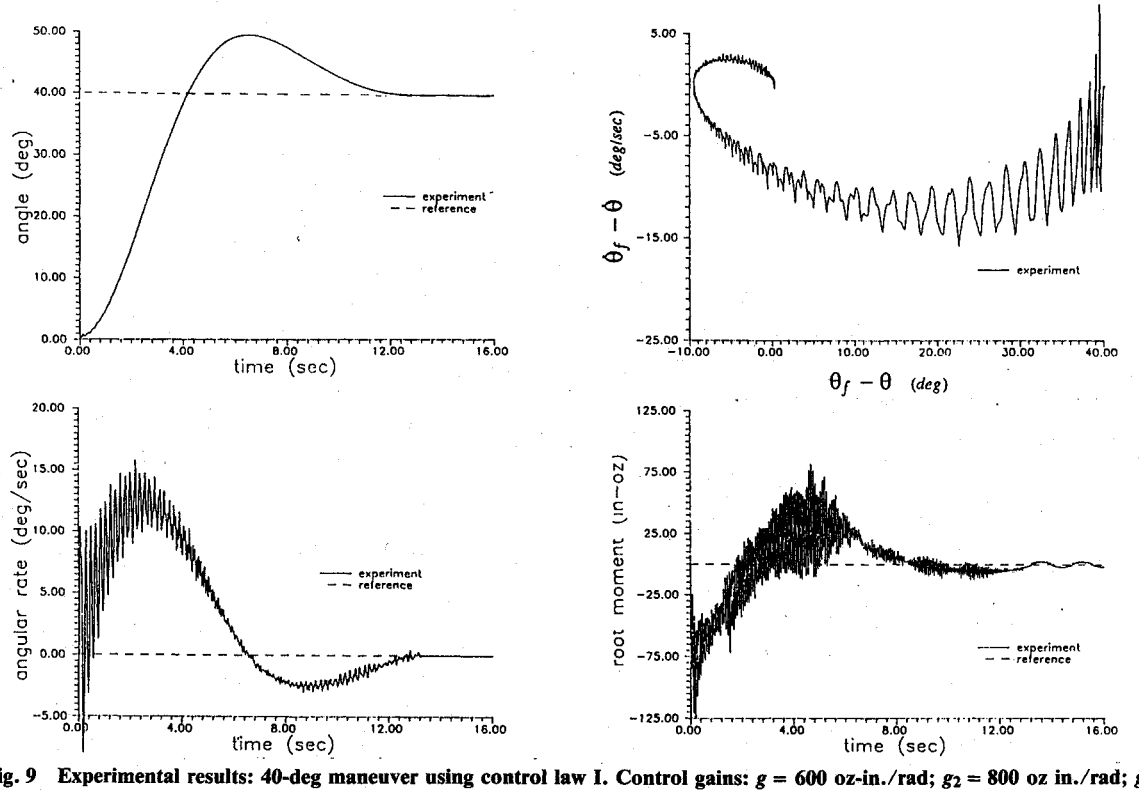

Fig. 9 Experimental results: 40-deg maneuver using control law I. Control gains: g = 600 oz-in./rad; g_2 = 800 oz in./rad; g_3 = 0.

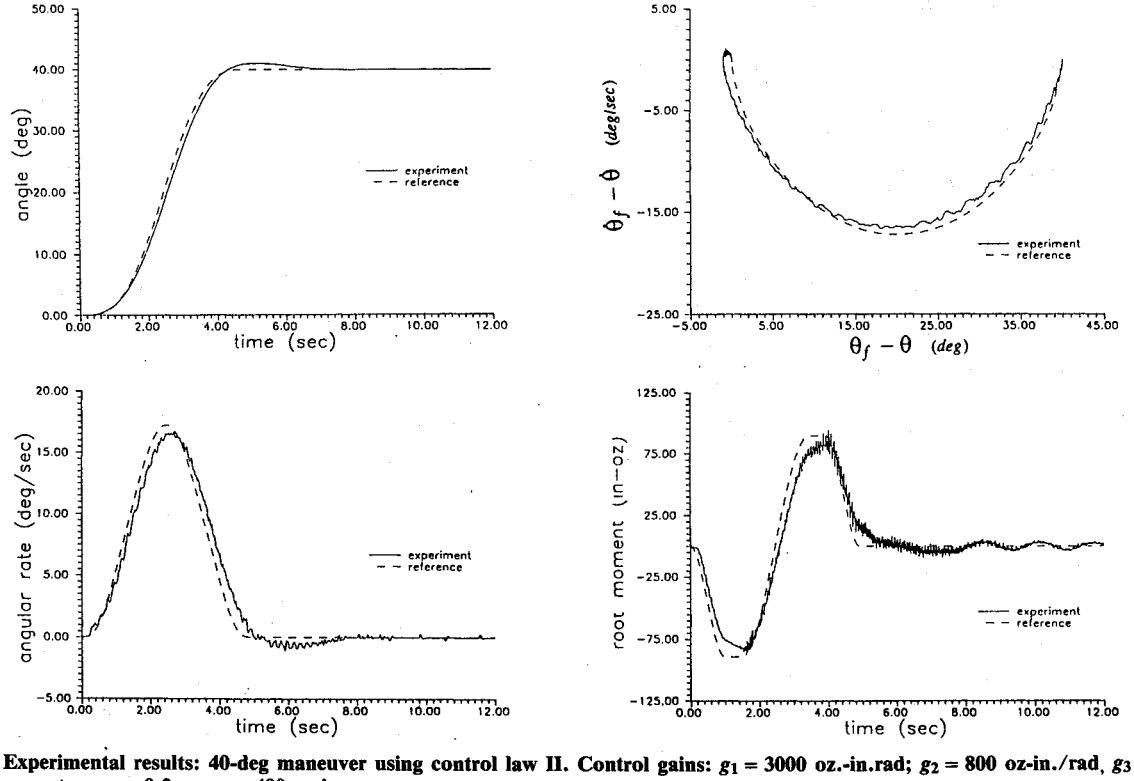

Fig. 10 Experimental results: 40-deg maneuver using control law II. Control gains: g_1 = 3000 oz.-in.rad; g_2 = 800 oz-in./rad, g_3 = 0. Torque-shaped parameters: α = 0.2, $u_{\max}$ = 400 oz-in.

ing torque for moderate $\dot{\theta}$ and is about 5% of the peak commanded torque of 400 oz-in. Although we believe Eq. (23) models the bearing friction well, we found that it is difficult to use this model to compensate for bearing friction in real time because angle encoder noise results in our estimated instants that $\dot{\theta}$ switches sign being uncertain. This difficulty has significant practical consequences. If we modify our control using Eq. (23), the commanded discontinuity (at the estimated time that $\dot{\theta}$ changes sign) will not coincide exactly with the actual stiction discontinuity; even slightly mistimed compensation torque discontinuities can actually worsen the disturbance! Although we experimented with several bearing torque compensation schemes, we ultimately decided to simply consider bearing torque an anticipated and well-modeled disturbance. Our simulations (such as the results shown in Fig. 8) indicated that our control approach could easily tolerate disturbances of this magnitude, and our successful experiments in Figs. 9, 10, and Ref. 2 certainly confirm that our implemented control laws are robust in the presence of the actual disturbances.

Concluding Remarks

We have presented an approach to the design of feedback control laws for large maneuvers of distributed parameter systems and have conducted successful experiments. This approach establishes stable gain regions over which subsequent optimizations can be carried out with global stability guaranteed (to within model errors, of course). The formulation permits approximate imposition of actuator saturation constraints and a priori control shaping via user specification of a torque-shaped, optimized reference trajectory. The resulting track-type control law is shown to result in Lyapunov stability in the sense that all trajectories are globally attracted to a small region near the reference trajectory. The tracking law automatically blends smoothly into a globally stable, constant gain, terminal output feedback controller. We believe this approach is much more attractive than gain scheduling because the logical and implementation complications associated with discontinuous gain change (handoff) logic can be avoided altogether. We have considered in detail the case of single axis maneuvers of a flexible body system and a particular family of torque-shaped, near-minimum-time rigid body reference trajectories. We demonstrated numerically the effects of torque shaping on maneuver time and established a precomputable bound on the size of region near the target trajectory in which Lyapunov-stable tracking cannot be guaranteed. We described hardware experiments that successfully implemented these ideas.

We have demonstrated the feasibility of our analytical formulations and experimental approach. We are optimistic that these ideas extend to a significant family of multiaxis maneuvers of multiple flexible body systems and the maneuver control problems associated with multiple body reconfiguration, pointing/tracking, and deployment dynamics.

Acknowledgments

The support of the Air Force Office of Scientific Research, Contract F49620-87-C-0078, and A. K. Amos is appreciated. We also received support from the Texas Advanced Technology Program, Project 70110. The authors are pleased to acknowledge the work of H. Fujii, S. R. Vadali, and A. Das; their earlier research provided inspiration for this work. We also thank the following individuals for their contributions: T. C. Pollock for his significant contributions to all aspects of the design and development of the experiment hardware, Steve Morgan for identifying the structural parameters and for his assistance with the angle encoder, Johnny Hurtado for his assistance in carrying out the experiments, and Becky Masters for excellent support in preparing this manuscript.

References

[1]Junkins, J. L., and Turner, J. D., *Optimal Spacecraft Rotational Maneuvers,* Elsevier, Amsterdam, The Netherlands, 1986.

[2]Junkins, J. L., Rahman, Z., and Bang, H., "Near-Minimum-Time Maneuvers of Flexible Vehicles: A Liapunov Control Law Design Method," AIAA Paper 90-1222, April 1990.

[3]Wie, B., Weiss, H., and Arapostathis, A., "Quaternion Feedback for Spacecraft Eigenaxis Rotations," *Journal of Guidance, Control, and Dynamics,* Vol. 12, No. 3, 1989, pp. 375–380.

[4]Juang, J.-N., Horta, L. G., and Robertshaw, J. H., "A Slewing Control Experiment for Flexible Structures." *Proceedings of the Fifth VPI & SU Symposium on Dynamics and Control of Large Structures,* Virginia Polytechnic Inst. and State Univ., Blacksburg, VA, June 1985, pp. 547–551.

[5]Fujii, H., Ohtsuka, T., and Udou, S., "Mission Function Control for Slew Maneuver Experiment." *Journal of Guidance, Control, and Dynamics*, Vol. 12, No. 6, 1989, pp. 858–865.

[6]Junkins, J., Rahman, Z., Bang, H., and Hecht, N., "Near-Minimum-Time Feedback Control of Distributed Parameter Systems: A Liapunov Control Law Design Method," *Proceedings of the Seventh VPI and SU Symposium on Dynamics and Control of Large Structures,* Virginia Polytechnic Inst. and State Univ., Blacksburg, VA (to be published).

[7]Rahman, Z., Junkins, J. L., Pollock, R. C., and Bang, H., "Large Angle Maneuvers with Vibration Suppression: Analytical and Experimental Results," *Seventh VPI and SU Symposium on Dynamics and Control,* Virginia Polytechnic Inst. and State Univ., Blacksburg, VA (to be published).

[8]Thompson, R.C., Junkins. J. L., and Vadali, S. R., "Near-Minimum-Time Open-Loop Slewing of Flexible Vehicles," *Journal of Guidance, Control, and Dynamics*, Vol. 12, No. 1, 1989, pp. 82–88.

[9]Vadali, S. R., "Feedback Control of Flexible Spacecraft Large Angle Maneuvers Using Liapunov Theory," *Proceedings of the 1984 American Control Conference,* Inst. of Electrical and Electronics Engineers, Piscataway, NJ, June 1984, pp. 1674–1678.

[10]Byers, R. M., Vadali, S. R., and Junkins, J. L., "Near-Minimum-Time Closed-Loop Slewing of Flexible Spacecraft." *Journal of Guidance, Control, and Dynamics,* Vol. 13, No. 1, 1990, pp. 57–65.

[11]Meirovitch, L., and Quinn, R., "Maneuvering and Vibration Control of Flexible Spacecraft," *Journal of the Astronautical Sciences,* Vol. 35, No. 3, 1987, pp. 301–328.

[12]Singh, G., Kabamba, P., and McClamroch, N., "Planar Time Optimal Slewing Maneuvers of Flexible Spacecraft," *Journal of Guidance, Control, and Dynamics*, Vol. 12, No 1, 1989, pp. 71–81.

[13]Breakwell, J. A., "Optimal Feedback Control for Flexible Spacecraft," *Journal of Guidance, Control, and Dynamics,* Vol. 4, No. 5, 1981, pp. 427–479.

[14]VanderVelde, W., and He, J., "Design of Space Structure Control Systems Using On-Off Thrusters," *Journal of Guidance, Control, and Dynamics,* Vol. 6, No. 1, 1983, pp. 759–775.

[15]Thompson, R. C., "A Perturbation Approach to Control of Rotational/Translational Maneuvers of Flexible Space Vehicles," M.S. Thesis, Engineering Mechanics, Virginia Polytechnic Inst. and State Univ., Blacksburg, VA, April 1985.

[16]Morgan, S. E., "Identification and Open-Loop Control of a Flexible Space Structure," M.S. Thesis, Aerospace Engineering, Texas A&M Univ., College Station, TX, Dec. 1989.